Acknowledgment. We thank Prof. P.-G. de Gennes for a useful discussion. This study was performed with financial support from the "Piano Finalizzato per la Chimica Fine e Secondaria", CNR, Italy.

Registry No. Polystyrene, 9003-53-6.

References and Notes

(1) O. B. Ptitsyn, A. K. Kron, and Y. Y. Eizner, *J. Polym. Sci., Part C*, **16**, 3509 (1968).
(2) P.-G. de Gennes, *J Phys. (Paris), Lett.*, **36**, L55 (1975).
(3) I. M. Lifshitz, *Sov. Phys.—JETP (Engl. Transl.)*, **28**, 1280 (1969).
(4) Y. Y. Eizner, *Polym. Sci. USSR (Engl. Transl.)*, 11, 409 (1979).
(5) I. C. Sanchez, *Macromolecules*, **12**, 980 (1979).
(6) I. M. Lifshitz, A. Y. Grosberg, and A. R. Khokhlov, *Rev. Mod. Phys.*, **50**, 683 (1978).
(7) G. Allegra, *Macromolecules*, **16**, 555 (1983).
(8) G. Allegra and F. Ganazzoli, *J. Chem. Phys.*, **76**, 6354 (1982).
(9) M. Nierlich, J. P. Cotton, and B. Farnoux, *J. Chem. Phys.*, **69**, 1379 (1978).
(10) S. T. Sun, I. Nishio, G. Swislow, and T. Tanaka, *J. Chem. Phys.*, **73**, 5971 (1980).
(11) R. Perzinski, M. Adam, and M. Delsanti, *J. Phys. (Paris)*, **43**, 129 (1982).
(12) C. Cuniberti and V. Bianchi, *Polymer*, **15**, 346 (1974).
(13) H. Yamakawa, "Modern Theory of Polymer Solutions", Harper and Row, New York, 1971, Chapter 3.
(14) P. J. Flory, *J. Chem. Phys.*, **17**, 303 (1949).
(15) A. R. Khokhlov, *J. Phys. (Paris)*, **38**, 845 (1977).
(16) P. Corradini, G. Natta, P. Ganis, and P. A. Temussi, *J. Polym. Sci., Part C*, **16**, 2477 (1967).
(17) G. Weill and J. des Cloizeaux, *J. Phys. (Paris)*, **40**, 99 (1979).
(18) P.-G. de Gennes, *J. Phys. (Paris), Lett.*, **39**, L298 (1978).
(19) A. Webman, J. L. Lebowitz, and M. H. Kalos, *Macromolecules*, **14**, 1495 (1981).

Conformational Characteristics of Polyisobutylene

Ulrich W. Suter,† Enrique Saiz,‡ and Paul J. Flory*

IBM Research Laboratory, San Jose, California 95193. *Received January 17, 1983*

ABSTRACT: The intramolecular energy of segments in a poly(1,1-dimethylethylene) chain (PIB) has been estimated by calculations on structures CH_3–$[C(CH_3)_2CH_2]_x$–H, with $x = 2$ (dimer), 3 (trimer), and 4 (tetramer), and on a hexad of structure CCH_2–$[C(CH_3)_2CH_2]_6$–C. PIB chains are subject to large steric repulsions that computations on analogues of low molecular weight do not properly take into account since the steric strain is relieved at the chain ends. We introduce an *iterative scheme* that eliminates end effects and correctly estimates the effects of steric strain on the configuration of the long-chain PIB molecule. Strain energy estimations for 2,2,4,4-tetramethylpentane, as well as for a diad in a long PIB chain, agree well with experimental values. The two-bond repeat regular conformation of lowest computed energy is an 8_3 helix, with helix parameters in excellent agreement with the conformation in crystalline PIB according to X-ray crystallographic results. The detailed analysis of all diad, triad, and tetrad conformations and of more than 100 conformations for the hexad is complex; the steric stress in PIB chains is manifested in interactions that are transmitted beyond nearest neighbors. In good approximation, however, the significant conformations of PIB can be represented by a four-state rotational isomeric scheme, with only one adjustable statistical weight parameter. Rotational isomeric states are located at +15° (t_+), −15° (t_-), +130° (g_+^+), and −130° (g_-^+). Skeletal ∠CCC bond angles are 123° at the methylene groups and 109° at the quaternary carbon atoms. Conformations divide into a "+ class" and a "− class". Bond conformations tend to be followed by those from the same class, changes from one to the other being rare. The characteristic ratio and its temperature coefficient, computed with the four-state scheme, agree well with experimental values.

Introduction

Poly(1,1-dimethylethylene), or polyisobutylene (PIB), is a prominent example of symmetrically substituted vinylidene chains. Its constitution, represented by

$$CH_3\text{–}[C(CH_3)_2CH_2]_x\text{–}H$$

is simple, and reliable experimental results on the molecular conformation in the crystalline state and in solution are available. Nevertheless, no satisfactory theoretical model for the conformational characteristics of this polymer has been presented heretofore.

The crystal structure of PIB has been studied by several investigators using X-ray fiber diagrams.[1-6] At present, there is general agreement that PIB assumes an 8_3 helix in the crystalline state,[4-7] distorted somewhat to allow for denser packing into an orthorombic unit cell.[6,7] The average skeletal bond angles are quoted[6,7] as ∠C–CH_2–C $\approx 128°$ and ∠CH_2–C–CH_2 $\approx 110°$ and the average torsion angles as ca. 125° and 15° (relative to the trans conformation).

Principal results on the spatial configuration of the PIB chain consist of the unperturbed chain dimensions and their temperature coefficient. Measurement of the intrinsic viscosities of samples spanning a wide range of molecular weights carried out in two considerably different Θ-solvents, benzene[8,9] and isoamyl valerate,[10] yielded characteristic ratios C_∞ in the range $6.6 \leq C_\infty \leq 6.9$ at ca. 300 K. The temperature coefficient $d \ln C_\infty/dT$ has been determined from stress–temperature measurements at constant pressure[11] as well as at constant volume[12] on samples of cross-linked PIB (butyl rubber) and from the temperature dependence of the intrinsic viscosity in *n*-hexadecane.[13] Between 291 and 368 K the temperature coefficient assumes a small negative value of ca. −0.2 (±0.2) $\times 10^{-3}$ K^{-1}. Experimental results on C_∞ and $d \ln C_\infty/dT$ are listed in Table I.

Several theoretical studies of the conformational characteristics of randomly coiled PIB chains have been reported.[5,14-21] Early attempts[14-16] were carried out under the assumptions that the bonds within a diad are restricted to torsion angles similar to the ones believed at the time to occur in the helical conformations of crystalline PIB and that neighboring diads are essentially uncorrelated. Subsequent examination[5,17] indicated these models to be oversimplified and that additional rotational states should

†Permanent address: Department of Chemical Engineering, Massachusetts Institute of Technology, Cambridge, MA 02139.
‡Permanent address: Departamento de Quimica Fisica, Universidad Alcalá de Henares, Alcalá de Henares (Madrid), Spain.

0024-9297/83/2216-1317$01.50/0

Table I
Experimental Values of Characteristic Ratios and Their Temperature Coefficients for PIB

T, K	C_∞[a]	$10^3 d \ln C_\infty/dT$[b]	ref	remarks
297	6.6		8	Θ-point, benzene, $[\eta]$
297	6.6 ± 0.1		9	Θ-point, benzene, $[\eta]$
295	6.9		10	Θ-point, isoamyl valerate, $[\eta]$
293-368		−0.08 (±0.10)	11	bulk, $(\partial f/\partial T)_p$
293-333		−0.09 (±0.08)	11	swollen, *n*-hexadecane, $(\partial f/\partial T)_p$
291		−0.26 (±0.10)	12	bulk, $(\partial f/\partial T)_v$
303-403		ca. −0.28	13	*n*-hexadecane, d ln $[\eta]/dT$

[a] Calculated from $[\eta]$ with $\Phi = 2.6 \times 10^{21}$. [b] Limits are standard deviations.

be taken into account. Allegra et al.[5] allowed for deformation of ∠C–C–C bond angles and computed the preferred helical (±0.2) in close agreement with experiment.[4-7] They represented the conformations of the random chain by a simple three-state scheme derived from energies calculated for helical chains, i.e., subject to the restriction that rotation angles within every diad are the same. Energies calculated on this basis are not strictly applicable to random chains, however.

Surprisingly, theoretical calculations based on the simplified schemes briefly indicated yielded values for C_∞ in agreement with experiment.[5,14-16,21] Rejecting inferences from the conformation of the preferred helix, Boyd and Breitling[19] carried out elaborate calculations on model compounds of PIB, i.e., on a dimer, a trimer, and a tetramer model, taking into account interactions between all atoms and allowing for distortion of all angles and even of bond lengths. They found that a six-state rotational isomeric state scheme would represent the conformational potential hypersurfaces in good approximation. The characteristic ratio computed with their scheme was only 4.6, however (compare Table I).

In this paper, we examine the conformational energies of model compounds and of segments of a PIB chain containing up to six monomeric units. Conformational energies have been calculated as functions of the skeletal conformations by using empirical potentials for nonbonded interactions that are validated by results on low molecular weight hydrocarbons; all bond angles and torsion angles (other than those specified for the chosen pair of skeletal bonds) were relaxed to minimize the total energy. The calculations lead to a rotational isomeric state scheme that departs drastically from those proposed previously. Characteristic ratios and their temperature coefficients, calculated according to this scheme, are compared with experimental results.

Conformational Energies

Parameters for the Calculation of Conformational Energies. The conformational energy was calculated as the sum of three terms: (i) intrinsic torsional energy, (ii) energies of bond angle deformations, and (iii) interaction energies between pairs of nonbonded atoms.

A threefold intrinsic torsional energy function with a barrier of 2.8 kcal mol^{-1} was assigned to each C–C bond.[22] Bond angle deformation energies were treated in the harmonic approximation $E_\theta = \sum(k_\theta/2)(\theta - \theta_0)^2$, all bond angles being included in the sum. Values for k_θ and θ_0 for the different types of bond angles occurring in PIB, i.e., ∠C–C–C, ∠C–C–H, and ∠H–C–H, are taken from ref 23 and are listed in Table II. Bond lengths were kept constant.

Nonbonded interactions between atoms separated by more than two bonds were estimated using a spliced, three-piece pair energy function. This function, previously used to estimate the conformational characteristics of poly(vinyl ketones),[24] takes account of the effect of surrounding molecules in a condensed phase on the pair interaction energies in rough approximation. When the distance r between two nonbonded atoms i and j is small, the energy is estimated by the traditional Lennard-Jones function $f_{6\text{-}12}(r) = (a_{ij}/r^{12}) - (c_{ij}/r^6)$. It is large and positive for small values of r and decreases with increasing interatomic distance until it reaches negative values and a minimum at $r = r_i^0 + r_j^0$, where the r_k^0 are the *adjusted* van der Waals radii of the atoms i and j. With further increase in the distance between atoms i and j, $f_{6\text{-}12}$ increases and approaches a value of zero asymptotically. In reality, the loss of attraction when the atoms are moved apart is compensated by interactions with the solvent as soon as the (intramolecular) interatomic distance is sufficient to create a "void" into which a solvent molecule can penetrate. When the distance between the two proximate atoms is larger than this critical distance, r^*, we therefore hold the nonbonded interaction energy constant at $f_{6\text{-}12}(r^*)$. To avoid a discontinuity in the first derivative of the energy function with respect to r (with a concomitant singularity in the second derivative with respect to r) a cubic polynomial is spliced between the Lennard-Jones 6–12 function and the plateau of constant energy for $r > r^*$. The cubic polynomial is chosen so that the energy and its first derivative are continuous at the junctions; it spans a distance h. On the "left side" the cubic joins the Lennard-Jones function at $r_l = r^* - h/2$, and on the "right side" it joins the plateau of constant potential at $r_r = r^* + h/2$. Thus,

$$r \le r_l: \qquad E = f_{6\text{-}12}(r)$$

$$r_l < r < r_r:$$

$$E = f'_{6\text{-}12}(r_l)[r_r - r]^2[r - r_l]/h^2 + f_{6\text{-}12}(r_l)[r_r - r]^2\{2[r - r_l] + h\}/h^3 + f_{6\text{-}12}(r^*)[r - r_l]^2\{2[r_r - r] + h\}/h^3$$

$$r \ge r_r: \qquad E = f_{6\text{-}12}(r^*) \qquad (1)$$

where $f'_{6\text{-}12}(r_l)$ is the first derivative of the Lennard-Jones function with respect to r at r_l, and $h = r_r - r_l$. Parameters chosen are listed in Table II. The critical distance r^* was set to 4.5 Å for calculations that model condensed-phase

Table II
Parameters Used in Energy Calculations

bond	bond length, Å	intrinsic torsional barrier, kcal mol^{-1}
C–C	1.53	2.8
C–H	1.10	
bond angle	**$10^3 k_\theta$, kcal deg^{-2} mol^{-1}**	**$\pi - \theta_0$, deg**
∠C–C–C	35.1	111
∠C–C–H	26.7	109.5
∠H–C–H	22.3	107.9
interacting pair	**$10^{-3} a_{ij}$, kcal mol^{-1} Å^{12}**	**c_{ij}, kcal mol^{-1} Å^6**
C,C	398.3	366.0
C,H	56.8	127.9
H,H	7.3	47.1

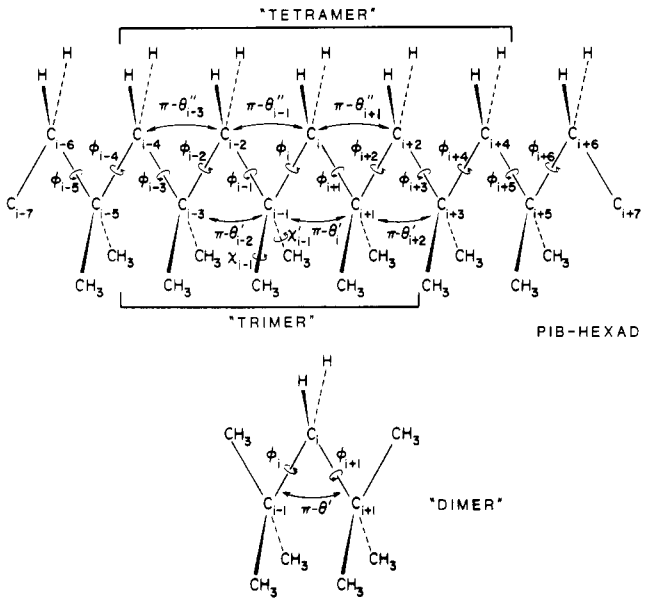

Figure 1. PIB models and sequences in PIB chains.

Table III
Torsional Barriers in Hydrocarbons

bond	barrier height, kcal mol^{-1} calcd	exptl[25]
CH_3-CH_3	3.08	2.9, 3.0
CH_3-C_2H_5	3.35	3.4
CH_3-$CH(CH_3)_2$	3.72	3.6, 3.9
CH_3-$C(CH_3)_3$	4.13	4.3
C_2H_5-C_2H_5	3.70	3.3, 3.6

situations and to $r^* \rightarrow \infty$ for comparison with gas-phase experiments. The range represented by the cubic polynomial was chosen to be $h = 1$ Å.

The composite potential functions thus defined were tested by calculating the barriers to rotation in simple hydrocarbons. Results of these calculations, together with experimental values,[22,25] are listed in Table III. Agreement between calculations and experiments is good.

In subsequent calculations, all torsion angles and bond angles were subject to change according to the requirements of the specific computation. All atoms were treated individually. Figure 1 displays a segment of the PIB chain comprising a hexad in its all-trans conformation (all skeletal torsion angles $\varphi = 0$). Torsion angles of methyl groups in front of the plane formed by the carbon–carbon backbone are denoted by χ, and those behind this plane by χ'. At $\chi_k = \chi_k' = 0$ a C–H bond of each pendant methyl group is trans with respect to skeletal bond k.

Conformational Energies for the Dimer. The "dimer" 2,2,4,4-tetramethylpentane was used as the simplest model for the central diad of the PIB chain (see Figure 1). Its conformational energy depends on eight torsion angles (φ_i, φ_{i+1}, plus six methyl torsion angles) and 45 independent bond angles θ (11 ∠C–C–C, 22 ∠C–C–H, and 12 ∠H–C–H). In order to simplify the representation of the conformational energy, we chose to compute the energy for given values of φ_i and φ_{i+1}, the values of all other angles being adjusted to minimize the energy for the pair of "skeletal" torsion angles selected. The resulting conformational energy can then be conveniently represented by contours in the φ_i, φ_{i+1} plane. Energy maps thus computed are very similar to those published by Allegra et al.[5] and are not shown here.

Minimization of the computed energy through adjustment of bond angles and torsion angles was achieved by quasi-Newton methods.[26] Two different algorithms were applied for the successive updating of the estimate of the Hessian matrix $\partial^2 E/\partial x_i \partial x_j$,[27,28] where x_k stands for any adjustable parameter. Fletcher's solution, available in the subroutine package VA10A,[28] proved most effective in reaching the minimum. This algorithm was employed in all further minimizations; frequent testing showed it to perform well in all cases treated here.

The calculations on 2,2,4,4-tetramethylpentane show that the energy minima are displaced ca. ±15° from the staggered positions (i.e., $\varphi = 0°, \pm 120°$) of the skeletal bonds. The pair of skeletal bonds within a given diad are constrained to adopt displacements of the same sign. These deductions agree with those of Boyd and Breitling,[19] who found displacements of ca. ±17°. In further agreement with these authors, we obtained 123° for the value of the skeletal bond angle $\pi - \theta'$ in the conformation of minimum energy, which compares favorably with the experimental value of 122.6° for the central C–CH_2–C angle in crystalline 2,2,4,4-tetramethyladipic acid.[29] The threefold symmetry of the *tert*-butyl moieties in the dimer model dictates that six torsional states be considered for a full rotation of φ_i or φ_{i+1}. These occur at ca. +15°, −15°, +135°, +105°, −105°, and −135°. Anticipating notation required for higher homologs, we designate them by t_+, t_-, g_+^+, g_-^+, g_+^-, and g_-^-, respectively. Energy minima for rotations of methyl groups occur close to $\chi \approx 0°$, the staggered form, for all skeletal conformations of the dimer. Departures from $\chi = 0°$ occur in some of the conformations of the higher homologs considered below, but they do not exceed |25°| for states of low energy.

The pairwise displacements of the minima from the staggered conformations are due to interlocking of the substituents to the quaternary carbons $i - 1$ and $i + 1$, which engage one another like a pair of cogwheels. This aspect of the conformational interactions in the PIB chain was recognized in earlier researches.[5,19] Conformations in which the two intradiad torsion angles have displacements of opposite sign, such as $|t_+t_-|$ (where the vertical bars designate the locations of the substituted quaternary carbon atoms), have energies in excess of 10 kcal mol^{-1} above $|t_+t_+|$. Hence, they may be ignored. We therefore formulate a simple selection rule according to which conformations $|\zeta_+\eta_-|$ and $|\zeta_-\eta_+|$ within a *diad* are forbidden; i.e., their statistical weights approach zero. Here ζ and η stand for t, g^+, or g^-.

As a test of the computations, we calculated the strain energy of the dimer model compound by taking the difference between the minimum energy for $|t_+t_+|$ and the minimum energy obtained when nonbonded interactions between methyl groups on C_{i-1} and on C_{i+1} are ignored (at $\varphi_i = \varphi_{i+1} \simeq 0$). We thus obtain $\Delta E = 6.5$ kcal mol^{-1} for the excess energy due to strain. This is in good agreement with the value of 6.6 kcal mol^{-1} that follows from heat of formation data, as Boyd and Breitling[19] showed.

Conformational Energies for the Trimer. The appropriate model for a triad in PIB is 2,2,4,4,6,6-hexamethylheptane. A representation of this molecule is afforded by Figure 1 if the sequence spanned by the brackets labeled "trimer" is separated from the PIB-hexad and hydrogen atoms are substituted for carbon atoms C_{i-5} and C_{i+3}. In order to evaluate conformational energies of the trimer, the following procedure was used: (i) one of the 36 possible combinations of states for bonds $i - 1$ and i was chosen (e.g., $t_+ |g_+^+|$); (ii) bonds $i - 2$ and $i + 1$ were set to t_+ or t_-, so that they would conform in sign to the state of their neighbors within the same diad (yielding, e.g., $|t_+t_+|g_+^+t_+|$), where, of course, the character t is completely

Table IV
Results from Energy Minimizations in the Trimer (Energy, kcal mol^{-1} [a]/(φ_{i-1}, φ_i/$\pi - \theta''$) in degrees)

	$\|t_+$	$\|t_-$	$\|g_+^+$	$\|g_-^+$	$\|g_+^-$	$\|g_-^-$
$t_+\|$	2.94 (16, 16/103)	3.63 (13, −13/104)	0 (15, 129/111)	1.24 (16, 109/110)	1.20 (15, −98/109)	1.93 (6, −126/112)
$t_-\|$	3.63 (−13, 13/104)	2.94 (−16, −16/103)	1.93 (−6, 126/111)	1.20 (−15, 98/109)	1.24 (−16, −109/110)	0 (−15, −129/m)
$g_+^+\|$	0 (129, 15/111)	1.93 (126, −6/112)	>8	3.86 (124, 104/118)	>8	>8
$g_-^+\|$	1.24 (109, 16/110)	1.20 (98, −15/109)	3.86 (104, 124/118)	2.52 (107, 107/117)	>8	>8
$g_+^-\|$	1.20 (−98, 15/109)	1.24 (−109, −16/110)	>8	>8	2.52 (−107, −107/117)	3.86 (−104, −124/118)
$g_-^-\|$	1.93 (−126, 6/112)	0 (−129, −15/111)	>8	>8	3.86 (−124, −104/118)	>8

[a] Energies are given relative to $t_+|g_+^+$ per mole of trimer.

arbitrary for the description of the conformation of bonds $i - 2$ and $i + 1$, the terminal *tert*-butyl groups being of threefold symmetry; and (iii) the bond and torsion angles were allowed to "relax" to the structure of minimum energy within the domain of the conformation specified for bonds $i - 1$ and i. In some domains, such as $g_+^+|g_+^-$, apparently no conformational energy minimum exists; i.e., nowhere are all partial first derivatives zero and all partial second derivatives positive. In these cases, all of which were of very high relative energy, the lowest energy found along the boundaries of the the domain (located at the nearest staggered conformation and at +60° or −60° therefrom for each of the six states) was taken to represent the domain.

Results of these calculations are summarized in Table IV. The following conclusions can be drawn immediately:

(i) Conformations $g^+|g^-$ and $g^-|g^+$ are of high energy, regardless of the subscripts denoting the signs of departure from staggered conformations of the backbone. Severe overlaps between methyl substituents to C_{i-3} and C_{i+1} (see Figure 1) are responsible for these high energies. They correspond to the classical "pentane" effect in alkanes, but the overlap energies are much higher due to the bulkiness of the terminal *tert*-butyl groups. These conformations will be disregarded.

(ii) Conformations $g_\pm^\pm|g_\pm^\pm$ and $g_-^-|g_-^-$ are of very high relative energy because of a similarly severe overlap of methyl groups attached to atoms C_{i-3} and C_{i+1}, as is immediately obvious from models. If we take, for instance, $\pi - \theta''_{i-1}$ to be 123°, all other bond angles to be tetrahedral, and $\varphi(g_\pm^\pm)$ = 135°, the distance between the two closest methyl groups in $g_\pm^\pm|g_\pm^\pm$ is only 1.33 Å. These conformations will be neglected also.

(iii) Inspection of Table IV suggests that *interdiad* interactions may be more important in determining conformational characteristics than the *intradiad* interactions, the latter having been noted in the dimer; see above. The resulting hierarchy of interactions contrasts with that prevailing in monosubstituted vinyl polymers. If we set an (arbitrary) cutoff level at 2 kcal mol^{-1} above $t_+|g_\pm^\pm$ and exclude from consideration all conformations of higher energy, then only $t|g$ (and $g|t$) conformations remain; cf. seq.

Our calculations yield energy differences at the minima that are roughly twice Boyd and Breitling's[19] values, but the rank of the different conformations is generally the same. The only exception is $g_-^+|g_-^\pm$ (and $g_+^-|g_+^-$) for which they estimate an energy of only 0.5 kcal mol^{-1} above $t_+|g_\pm^\pm$ while we obtain ca. 2.5 kcal mol^{-1}. The energy functions used here differ from those employed by Boyd and Breitling in that the nonbonded repulsions are "harder" and the atoms are assigned somewhat smaller radii. The H–H interaction, which is predominantly important in PIB, is here characterized by a minimum pair energy of −76 cal mol^{-1} at 2.6 Å and by +4900 cal mol^{-1} at 1.8 Å whereas Boyd and Breitling's function yields a minimum of −10 cal mol^{-1} at 3.3 Å and reaches +2300 cal mol^{-1} at 1.8 Å. Boyd and Breitling's procedure differs from ours also in disregarding interactions with neighboring (solvent) molecules; see above. Their calculations therefore ascribe higher energies to expanded conformations through failure to consider the inevitable compensation by neighboring molecules. Hence, compact conformations such as $g|g$ are artificially favored.

"End Effects" and Preliminary Calculations on the Tetramer. Closer inspection of the results briefly summarized above reveals that the skeletal bond angles at the terminal *tert*-butyl moieties, i.e., at C_{i-1} and C_{i+1} in the dimer and at C_{i-3} and C_{i+1} in the trimer, differ by several degrees from the corresponding values at C_{i-1} in the trimer. In the $|t_+t_+|t_+t_+|$ conformation of the trimer, for instance, $\pi - \theta''_{i-3} = \pi - \theta''_{i+1}$ is ca. 106° compared with 103° for $\pi - \theta''_{i-1}$. This feature was documented by Boyd and Breitling.[19] It can be attributed to the "stress" created in the structures by "crowding", i.e., to the fact that many atoms are brought into close proximity where their nonbonded repulsions are large. This "stress" can be relieved somewhat by distortions at the chain termini. The difference between the C–C–C bond angles for the skeletal bonds in the termini (which are always t_+) and the internal ones is an indication of this distortion.

Calculations on finite sequences of units invariably are affected by these end effects. In order to circumvent them and thus arrive at results relevant to diads situated within a long chain and remote from chain ends, we devised the following iterative procedure. All diads of a tetramer or hexamer (cf. seq.) sequence were assigned the same nominal conformation (e.g., $|t_+g_\pm^\pm|$), and all angles were relaxed to minimize the total energy. The angles defining the configuration of the central diad were then assigned to the terminal diads of the sequence. With these parameters fixed, those for the central diad were relaxed to minimize the energy. The resulting parameters were then assigned to the terminal diads, and the process was repeated until convergence was attained. Criteria chosen for convergence were constancy of angles within ±0.005° and of the total energy within ±1 cal (mol diads)$^{-1}$. Convergences within these narrow limits required fewer than twenty iterations.

It will be apparent that results obtained by the procedure indicated must match those for an internal diad within a very long sequence, all diads being in the chosen nominal conformation. The procedure is limited, of course, to regular (i.e., helical) conformations. Those nonregular conformations that are significant may be evaluated, however, by assigning a chosen conformation to the central

Table V
Results of the Iterative Scheme for Helical Conformations

conformation of hexad	energy per diad[a] $E_{tot}/5$, kcal mol^{-1}	angles, deg				helix parameters		helix form
		φ_i	φ_{i+1}	$\pi - \theta'$	$\pi - \theta''$	α, deg	d, Å	
$(\lvert t_+t_+)_5\rvert$ or $(t_+\lvert t_+)_6$	3.53	16.0	16.0	128.2	105.0	35.6	1.968	ca. 10_1
$(\lvert t_+g_+^+)_5\rvert$ or $(t_+\lvert g_+^+)_6$	0	15.1	129.4	124.6	109.3	137.1	2.261	8_3
$(\lvert t_+g_+^-)_5\rvert$ or $(t_+\lvert g_+^-)_6$	4.08	3.4	−103.3	127.5	109.2	−102.8	2.189	
$(\lvert g_-^+g_-^+)_5\rvert$ or $(g_-^+\lvert g_-^+)_6$	7.06	102.5	102.5	127.2	109.4	168.6	2.195	ca. 8_4
			experiment[b]			135.0	2.329	8_3

[a] Relative to the energy of $(\lvert t_+g_+^+)_5\rvert$ or $(t_+\lvert g_+^+)_6$. [b] The experimental values correspond to an 8_3 helix ($\alpha = 3 \times 2\pi/8$) with an axial repeat distance of 18.63 Å ($d = 18.63/8$); see ref 1 and 6.

diad situated between outer diads having conformations deduced for regular sequences in the foregoing manner. A single minimization step is then required. The configurations of the flanking diads in the real chain may be vitiated by the conformations of their neighbors to some extent. Secondary effects of this nature are here ignored. The results indicate them to be small.

Preliminary calculations with the iterative scheme were carried out for 2,2,4,4,6,6,8,8-octamethylnonane, represented in Figure 1 by the segment between brackets labeled "tetramer", with hydrogen atoms replacing carbon atoms C_{i-1} and C_{i+5}. Regular helical conformations with a two-bond repeat were first considered. An arbitrary configuration was assigned with $\varphi_{i-2} = \varphi_{i+2}$ and $\varphi_{i-1} = \varphi_{i+1} = \varphi_{i+3}$, all bond and torsion angles that are superposable by a corresponding shift in the index being equal. The total energy was then minimized with respect to the central diad, consisting of C_{i-1}, C_i, C_{i+1}, and all methyl groups and hydrogen atoms attached to them, by relaxation of all bonds and torsion angles associated with the central diad. The values of these angles were then assigned to the terminal diads; i.e., $\varphi_i \rightarrow \varphi_{i-2}$ and φ_{i+2}, $\varphi_{i+1} \rightarrow \varphi_{i-1}$ and φ_{i+3}, $\theta'_i \rightarrow \theta'_{i-2}$ and θ'_{i+2}, $\theta''_{i-1} \rightarrow \theta''_{i-3}$ and θ''_{i+3}, etc. The configuration of the central diad was again minimized, the adjusted values were carried outwards to the terminal diads, and so on until convergence within the limits quoted above was achieved.[30]

Calculations on hexads yielded similar results. Differences were minor; hence separate discussion of the two sets of results is unnecessary. Use of the hexad instead of the tetramer offers advantages as follows:

(i) Possible artifacts of the iterative scheme can be examined by broadening the section that is allowed to be adjusted.

(ii) Residual end effects that remain because the energy functions cannot be factorized completely into contributions from "adjustable" and fixed sections are smaller per diad inasmuch as the hexad contains three internal diads instead of one in the tetramer.

The tetramer model was used to estimate the strain energy of a diad in an infinitely long PIB chain in a manner similar to the estimation of the strain energy for the dimer (see above). The preferred conformation of the tetramer is $g_+^+\lvert t_+g_+^+\rvert t_+$ (bonds $i-2$ and $i+3$ do not require specification) with $\varphi_i \simeq 15°$ and $\varphi_{i+1} \simeq 130°$ and $\pi - \theta'_i \simeq 125°$ and $\pi - \theta''_{i+1} \simeq 110°$. We then calculated the minimum energy in the same fashion, but ignored the interactions between the methyl groups attached to C_{i-1} and C_{i+1}, and found, at $\varphi_i = \varphi_{i+1} \simeq 1.5°$, a minimum energy 7.6 kcal mol^{-1} lower than in the complete computation. This value is in reasonable agreement with the "experimental value" of 6–7 kcal mol^{-1}.[31-35]

Conformational Energies for the Hexad. The structure of the hexad used in these calculations is shown in Figure 1. The initial computations were performed on regular, two-bond repeat conformations in which the angles in the central diad were minimized and the values of these angles were assigned to the outer structure, e.g., $\theta'_i \rightarrow \theta'_{i-6}$, θ'_{i-4}, θ'_{i-2}, θ'_{i+2}, θ'_{i+4}, and θ'_{i+6}, according to the iterative scheme introduced above. Results for the dimer suggest that only 18 diad conformations need to be taken into account. Of these, only six are independent; others are generated from this basic set according to the symmetry relations:

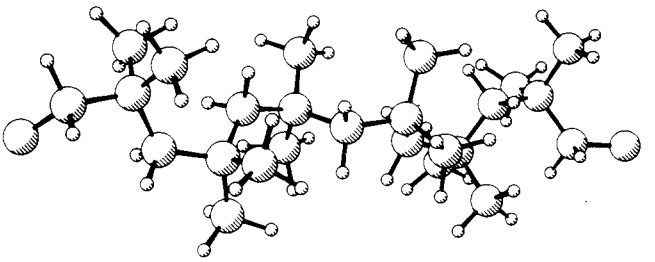

Figure 2. The conformation $(t_+\lvert g_+^+)_6$, or $(\lvert t_+g_+^+)_5\rvert$, obtained with the "iterative scheme". This corresponds to the 8_3 helical conformation found experimentally in the crystalline state.

$$\lvert t_+t_+\rvert \sim \lvert t_-t_-\rvert \tag{2a}$$

$$\lvert t_+g_+^+\rvert \sim \lvert g_+^+t_+\rvert \sim \lvert t_-g_-^-\rvert \sim \lvert g_-^-t_-\rvert \tag{2b}$$

$$\lvert t_+g_+^-\rvert \sim \lvert g_+^-t_+\rvert \sim \lvert t_-g_-^+\rvert \sim \lvert g_-^+t_-\rvert \tag{2c}$$

$$\lvert g_+^+g_+^+\rvert \sim \lvert g_-^-g_-^-\rvert \tag{2d}$$

$$\lvert g_+^+g_+^-\rvert \sim \lvert g_+^-g_+^+\rvert \sim \lvert g_-^-g_-^+\rvert \sim \lvert g_-^+g_-^-\rvert \tag{2e}$$

$$\lvert g_-^+g_-^+\rvert \sim \lvert g_+^-g_+^-\rvert \tag{2f}$$

The results obtained with the trimer further limit the helical conformations with a two-bond repeat to four, i.e., the conformations characterized by (2a), (2b), (2c), and (2f). These four regular conformations were treated by the iterative scheme; the results are given in Table V. Also included are the helix parameters, computed following Miyazawa,[36] where α is the rotation per monomeric unit about the helix axis and d the corresponding translation along the axis. The helical conformation with lowest energy, $(t_+g_+^+)_5$ or $(t_+\lvert g_+^+)_6$, depicted in Figure 2, is characterized by helix parameters that are in good agreement with crystallographic values;[1,6] the difference in α is less than 2% and in d it is less than 3%. All other two-bond repeat helical conformations are estimated to be more than 3 kcal (mol diads)$^{-1}$ higher in minimum energy, and their helix parameters do not match the ones observed.

The numerical accuracy of our procedures was tested by subjecting all symmetry-related conformations, indicated in eq 2a, 2b, 2c, and 2f, to the same iterative scheme, starting with nonsymmetric torsion angles and geometries. The energies of these eight additional conformations were all within ±0.001 kcal (mol diads)$^{-1}$ of the appropriate helix in Table V; all bond and torsion angles agreed within

±0.02°. The results presented evidently are not subject to artifacts of computational procedures.

In order to check if imposing a two-bond repeat regularity on the helical conformations might have caused artifacts in the results, a calculation for a four-bond repeat was performed using the iterative scheme for the preferred helix; i.e., the bonds φ_{i-1} and φ_{i+2} as well as the bond angles around atoms C_{i-2} and C_{i+2} were included in the "adjustable zone," and the adjusted values of bond angles and torsion angles were carried outward to the fixed termini after each minimization in accordance with the requirements for a four-bond repeat helix. Bond and torsion angles changed by less than 0.5° as a result of this procedure. A further calculation was performed by increasing the "adjustable zone" to a length of six skeltal C–C bonds; deviations in bond and torsion angles from the optimal configuration thus obtained and the one reported in Table V are less than 1.5°. The computations indicate that the exact way chosen to carry out the calculations with the iterative scheme is immaterial and that an 8_3 helix is indeed the regular two-bond repeat conformation that is strongly favored.

The results mentioned above do not imply, however, that no other helix, e.g., a *two-diad repeat* (a four-bond repeat) helix, is feasible. A conformation such as $(t_+|g_+^+g_+^+|t_+)_x$, similar to the one that occurs in syndiotactic vinyl polymers, for instance, could conceivably be of low energy. We estimated the energies of the regular conformations $(t_+|g_+^+g_+^+|t_+)_3$ and $(g_+^+|t_+t_+|g_+^+)_3$, by adapting the iterative scheme to the requirements of a four-bond repeat. The values for the energies of these two structures are 1.86 kcal (mol diads)$^{-1}$ for the first conformation and 0.34 kcal (mol diads)$^{-1}$ for the second one, compared with 0 for the preferred helix identified in Table V. (Direct comparison with the values in Table V must be made with caution, since the energies are results of minimizations on different "adjustable zones".) These two regular conformations cannot be ruled out by *intramolecular* considerations alone. In fact, even longer regular sequences having low conformational energies may conceivably exist. The rotational isomeric state scheme elaborated below implies that the two four-bond repeat conformations considered here are approximately equal in energy to the two-bond repeat regular conformation of lowest energy, provided that the "end effects" are correctly eliminated and that strict helical symmetry is not imposed on the chain.

The strategy outlined above was used to evaluate representative nonhelical conformations. For the outer diads, in general, only the two helical conformations with lowest energy were used, i.e., $(t_+|t_+)_x$ and $(t_+|g_+^+)_x$ and their equivalent forms (see eq 2). In some instances $(t_+|g_+^-)_x$ was used, but never $(g_-^+|g_-^+)_x$; the high energy of the latter, ca. 7 kcal mol^{-1}, renders its incidence negligible. Computations of the energies for 131 such arrangements were attempted with results documented in Table VI. Conformations 1 and 27 correspond to the two preferred helices from Table V. Energies reported are normalized to conformation 27, the one preferred in the crystal. Torsion angles at the central skeletal carbon atoms and bond angles for the central diad are reported. In 29 cases the final geometry after minimization did not remain in the domain assigned to that conformation at the outset, and changes in the starting geometry of the adjustable diad did not rectify this behavior. Entries are omitted in such instances.

As a check, corresponding calculations were carried out by minimizing the energy of the hexad in a regular conformation in one step, helical symmetry being imposed on the chain throughout the calculation. The geometries and conformations obtained by this *primitive scheme* were then used for the evaluation of the nonregular conformations. In this scheme, end effects are not eliminated; hence differences between the primitive and iterative schemes are an indication of the magnitude of the end effects. For conformations of low energy, the results obtained by the two methods were not more than 2 kcal mol^{-1} apart. In other instances, however, differences of up to 10 kcal mol^{-1} were observed, e.g., in conformation 126 in Table VI, for which the energy computed with the primitive scheme is only 15.2 kcal mol^{-1}.

It is clear from Table VI that $t|g$ is by far the most favored junction between diads. All conformations with relative energies below 2.5 kcal mol^{-1} have $t|g$ junctions exclusively.

Only energy minima have been considered thus far. Incorporation of the results shown in Table VI in a rotational isomeric state scheme requires, however, that the character of the energy hypersurface in the vicinity of each minimum also be taken into account. A full integration over the entire range of all variable angles (up to 39 in number) being impossible, we chose to represent the energy surface around the local minimum by a Taylor-series expansion, truncated after the term of second order, i.e., by

$$E(\mathbf{x}) = E_{\min} + \frac{1}{2!}\sum_{j,k=1}^{m}\left(\frac{\partial^2 E}{\partial x_j \partial x_k}\right)_{\min}(x_j - x_{j,\min})(x_k - x_{k,\min}) \quad (3)$$

where $\mathbf{x}$ is the vector of all m variables, φ, ξ, or θ. The (local) partition function in this harmonic approximation is

$$z = \int e^{-E(\mathbf{x})/RT}\,d\mathbf{x} = e^{-E_{\min}/RT}(2\pi RT)^{m/2}\left\{\det\left[\left(\frac{\partial^2 E}{\partial x_j \partial x_k}\right)_{\min}\right]_{jk}\right\}^{-1/2} \quad (4)$$

where $[\partial^2 E/\partial x_j \partial x_k]_{jk}$ is the Hessian matrix of all second derivatives. Since the factor $(2\pi RT)^{m/2}$ is the same for all conformations in Table VI, it can be dismissed. The last factor in eq 4 may then be identified with z_0 in the relation

$$z = z_0 \exp(-E_{\min}/RT) \quad (5)$$

The Hessian matrix can be computed in good approximation with modest computing effort even for systems with many dimensions. We employed a "seven-point formula" for the calculations[38] in which for the evaluation of $\partial^2 E/\partial x_j \partial x_k$ both variables must be stepped to values x, $x + \Delta$, and $x - \Delta$ in order to generate $E(0,0) \equiv (E_{\min})$, $E(\Delta,0)$, $E(0,\Delta)$, $E(\Delta,\Delta)$, $E(-\Delta,0)$, $E(-\Delta,-\Delta)$, and $E(0,-\Delta)$. The method requires only $m^2 + m + 1$ energy evaluations for m variables, and is accurate to order Δ^2. We let $\Delta = 1°$. The values for z_0 thus computed at the minimum energy positions for diads between fixed regular segments are included in Table VI.

Statistical Weights

Bond angles at the positions of minimum energy for different conformations vary considerably according to the results in Table VI. An equivalent statement applies to the torsion angles. The variations seem small enough, however, to warrant adoption of a rotational isomeric state (RIS) scheme, with states of individual bonds independent of those of neighbors, as a tentative approximation. Such a scheme offers major advantages of simplicity. Results obtained in the remainder of the paper justify the RIS procedure. If more accurate experimental data become

available at a later date it would be possible to reexamine the results in Table VI.

The conformations in Table VI can be approximated by a combination of rotational isomeric states centered at +15° (t_+), −15° (t_-), +130° (g_+^+), +105° (g_-^+), −105° (g_+^-), and −130° (g_-^-). With two exceptions, these states coincide with those found for the dimer; see above. First-order statistical weights taken relative to 1 for t_+ and t_- are denoted by σ for g_+^+ and g_-^- and σ' for g_-^+ and g_+^-. Focusing attention first on the intradiad matrix of statistical weights U'',[20] we use the traditional symbols ω for the second-order interaction CH_3/CH_3, ω' for CH_3/CH_2, and ω'' for CH_2/CH_2. Since every conformation of a PIB diad involves two second-order interactions, only the ratios of these statistical weights are required. Combining these ratios in the following parameters of mixed order

$$\alpha = \sigma\omega/\omega'$$
$$\beta = \sigma\omega'/\omega'' \qquad (6)$$
$$\beta' = \sigma'\omega'/\omega''$$

and including all first-order parameters in U″,[20] we obtain

$$\mathbf{U}'' = \begin{bmatrix} 1 & 0 & \beta & 0 & \beta' & 0 \\ 0 & 1 & 0 & \beta' & 0 & \beta \\ \beta & 0 & \beta^2 & 0 & \alpha\beta' & 0 \\ 0 & \beta' & 0 & (\beta')^2 & 0 & \alpha\beta' \\ \beta' & 0 & \alpha\beta' & 0 & (\beta')^2 & 0 \\ 0 & \beta & 0 & \alpha\beta' & 0 & \beta^2 \end{bmatrix} \qquad (7)$$

where the states are indexed in the order t_+, t_-, g_+^+, g_-^+, g_+^-, g_-^-.

With U″ so defined, the interdiad matrix of statistical weights U′ contains second-order parameters only. Unfortunately, neither inspection of models nor of the results in Table VI suggests similarities between any two of its elements, except for trivial symmetry. There are eight independent states in U′, and we therefore set it tentatively to

$$\mathbf{U}' = \begin{bmatrix} \gamma & \delta & 1 & \epsilon & \zeta & \xi \\ \delta & \gamma & \xi & \zeta & \epsilon & 1 \\ 1 & \xi & 0 & \rho & 0 & 0 \\ \epsilon & \zeta & \rho & \psi & 0 & 0 \\ \zeta & \epsilon & 0 & 0 & \psi & \rho \\ \xi & 1 & 0 & 0 & \rho & 0 \end{bmatrix} \qquad (8)$$

where the statistical weights are normalized to unity for $t_+|g_+^+$ and states equivalent thereto as dictated by eq 2. The matrix contains seven unknown parameters.

The final columns of Table VI give the numbers of the various statistical weights for each conformation of the hexad. The conformational energies E_η (where $\eta = \alpha, \beta, \beta', \ldots, \rho$) as well as the preexponential factors η_0 in the generic equation for the statistical weights

$$\eta = \eta_0 \exp(-E_\eta/RT) \qquad (9)$$

can be computed from the entries in Table VI since for each conformation the sum of all conformational energies must equal the energy E for that conformation in Table VI, and z_0 is the product of all η_0's associated with the "adjustable zone" of the hexad.[39] Thus, we have to solve two overdetermined systems of equations each in 11 unknowns (11 statistical weights inclusive of the state of reference) in order to obtain all E_η's and η_0's. The equations were solved by computing the generalized inverse of the matrix of coefficients of the equations, i.e., of the array of numbers given in Table VI. To investigate whether conformations of high energy, of which there are many, influence the results significantly, we performed the identical calculation with conformations of lower energy given greater weight than those of higher energy on the following basis: E_{min}(kcal mol^{-1}) ≤ 2 (factor 10), 2–4, (factor 8), 4–6 (factor 6), 6–8 (factor 4), 8–10 (factor 2), ≥10 (factor 1). The results of these calculations are given in Table VII; the indicated limits bracket the values for the E_η's obtained in the two calculations, weighted and unweighted. The total root-mean-square error of the weighted fit is 1.6 kcal mol^{-1} for the energies E_{min} of the 102 minima and 0.25 for the preexponential factors z_0. The error is much smaller for states of low energy.

The a priori probability that a bond in a long PIB chain assumes any one of the six conformational states can be deduced[40] from eq 7 and 8 and values of the statistical weights η available from the results in Table VII. The a priori probabilities thus calculated are

$$P = [0.250, 0.250, 0.250, <10^{-5}, <10^{-5}, 0.250] \quad \text{at 300 K} \qquad (10)$$

and

$$P = [0.250, 0.250, 0.250, <10^{-4}, <10^{-4}, 0.250] \quad \text{at 400 K} \qquad (11)$$

the states being indexed as in eq 7 and 8. These findings indicate that the states g_-^+ and g_+^- can be neglected. This leads to the four-state scheme discussed below.

The Four-State Scheme

Statistical Weight Matrices. Striking the fourth and fifth columns and rows in U′ and U″ yields the appropriate 4 × 4 matrices. In U″ only the parameter β remains, and it can be factored out for later convenience:

$$\mathbf{U}'' = \begin{bmatrix} 1 & 0 & \beta & 0 \\ 0 & 1 & 0 & \beta \\ \beta & 0 & \beta^2 & 0 \\ 0 & \beta & 0 & \beta^2 \end{bmatrix} =$$
$$\text{diag}(1,1,\beta,\beta) \begin{bmatrix} 1 & 0 & 1 & 0 \\ 0 & 1 & 0 & 1 \\ 1 & 0 & 1 & 0 \\ 0 & 1 & 0 & 1 \end{bmatrix} \text{diag}(1,1,\beta,\beta) \qquad (12)$$

The interdiad matrix U′ retains three statistical weight parameters, γ, δ, and ξ:

$$\mathbf{U}' = \begin{bmatrix} \gamma & \delta & 1 & \xi \\ \delta & \gamma & \xi & 1 \\ 1 & \xi & 0 & 0 \\ \xi & 1 & 0 & 0 \end{bmatrix} \qquad (13)$$

Both γ and δ are estimated to be smaller than 10^{-4} at 300 K, and smaller than 8×10^{-4} at 400 K (see Table VII). They may be set to zero, since neither of these parameters is multiplied with a large factor when U′ is pre- or post-multiplied with U″. Taking advantage of the factorization of U″ in eq 12 we reassign the parameter β to U′ and notice that

$$\text{diag}(1,1,\beta,\beta)\ \mathbf{U}'\ \text{diag}(1,1,\beta,\beta) = \beta\mathbf{U}' \qquad (14)$$

Equation 14 makes clear that β must occur *once per junction of two diads*. It can therefore by eliminated by renormalization.

The statistical weight matrices then take on their final forms

$$\mathbf{U}'' = \begin{bmatrix} 1 & 0 & 1 & 0 \\ 0 & 1 & 0 & 1 \\ 1 & 0 & 1 & 0 \\ 0 & 1 & 0 & 1 \end{bmatrix} \qquad (15)$$

and

$$\mathbf{U}' = \begin{bmatrix} 0 & 0 & 1 & \xi \\ 0 & 0 & \xi & 1 \\ 1 & \xi & 0 & 0 \\ \xi & 1 & 0 & 0 \end{bmatrix} \qquad (16)$$

Table VI
Results from Energy Minimization for the Hexad (Energies in kcal mol^{-1}, Angles in Degrees)

	hexad-conformation	E	z_0	φ_i	φ_{i+1}	$\pi-\theta'$	$\pi-\theta''_{i-1}$	$\pi-\theta''_{i+1}$	α	β	β'	γ	δ	ϵ	ζ	ξ	ρ	ψ
1	$t_+ t_+ \mid t_+ t_+ \mid t_+ t_+ \mid t_+ t_+ \mid t_+ t_+$	17.62	0.45	16	16	128	105	105	0	0	0	4	0	0	0	0	0	0
2	$t_+ t_+ \mid t_+ t_+ \mid t_+ t_+ \mid t_+ g_+^+ \mid t_+ g_+^+$	15.56	0.33	16	16	128	105	103	0	2	0	3	0	0	0	0	0	0
3	$t_+ t_+ \mid t_+ t_+ \mid t_+ t_+ \mid t_- t_- \mid t_- t_-$	18.63	0.64	20	9	128	105	105	0	0	0	3	1	0	0	0	0	0
4	$t_+ t_+ \mid t_+ t_+ \mid t_+ t_+ \mid t_- g_-^- \mid t_- g_-^-$	17.04	0.52	20	13	129	105	104	0	2	0	2	1	0	0	0	0	0
5	$t_+ t_+ \mid t_+ t_+ \mid t_+ t_+ \mid g_+^+ t_+ \mid g_+^+ t_+$	10.91	1.19	16	13	126	105	111	0	2	0	2	0	0	0	0	0	0
6	$t_+ t_+ \mid t_+ t_+ \mid t_+ t_+ \mid g_-^- t_- \mid g_-^- t_-$	13.89	3.25	16	1	127	104	113	0	2	0	2	0	0	0	1	0	0
7	$t_+ g_+^+ \mid t_+ g_+^+ \mid t_+ t_+ \mid t_+ g_+^+ \mid t_+ g_+^+$	2.53	0.79	14	16	127	111	103	0	4	0	1	0	0	0	0	0	0
8	$t_+ g_+^+ \mid t_+ g_+^+ \mid t_+ t_+ \mid t_- t_- \mid t_- t_-$	5.91	1.88	17	10	126	111	105	0	2	0	1	1	0	0	0	0	0
9	$t_+ g_+^+ \mid t_+ g_+^+ \mid t_+ t_+ \mid t_- g_-^- \mid t_- g_-^-$	4.03	1.20	17	13	127	111	104	0	4	0	0	1	0	0	0	0	0
10	$t_+ g_+^+ \mid t_+ g_+^+ \mid t_+ t_+ \mid g_+^+ t_+ \mid g_+^+ t_+$	-0.26	1.26	11	11	123	113	113	0	4	0	0	0	0	0	0	0	0
11	$t_+ g_+^+ \mid t_+ g_+^+ \mid t_+ t_+ \mid g_-^- t_- \mid g_-^- t_-$	1.82	1.08	20	6	123	112	115	0	4	0	0	0	0	0	1	0	0
12	$t_- t_- \mid t_- t_- \mid t_+ t_+ \mid t_+ g_+^+ \mid t_+ g_+^+$	16.58	0.62	16	16	128	105	105	0	2	0	2	1	0	0	0	0	0
13	$t_- t_- \mid t_- t_- \mid t_+ t_+ \mid t_- t_- \mid t_- t_-$	20.27	1.89	15	15	128	106	106	0	0	0	2	2	0	0	0	0	0
14	$t_- t_- \mid t_- t_- \mid t_+ t_+ \mid t_- g_-^- \mid t_- g_-^-$	18.53	0.91	16	17	129	106	104	0	2	0	1	2	0	0	0	0	0
15	$t_- t_- \mid t_- t_- \mid t_+ t_+ \mid g_-^- t_- \mid g_-^- t_-$																	
16	$t_- g_-^- \mid t_- g_-^- \mid t_+ t_+ \mid t_+ g_+^+ \mid t_+ g_+^+$	5.97	1.04	2	20	127	113	103	0	4	0	1	0	0	0	1	0	0
17	$t_- g_-^- \mid t_- g_-^- \mid t_+ t_+ \mid t_- g_-^- \mid t_- g_-^-$																	
18	$t_- g_-^- \mid t_- g_-^- \mid t_+ t_+ \mid g_-^- t_- \mid g_-^- t_-$																	
19	$g_+^+ t_+ \mid g_+^+ t_+ \mid t_+ t_+ \mid t_+ g_+^+ \mid t_+ g_+^+$	7.04	0.31	17	17	129	104	104	0	4	0	2	0	0	0	0	0	0
20	$g_+^+ t_+ \mid g_+^+ t_+ \mid t_+ t_+ \mid t_- g_-^- \mid t_- g_-^-$	8.41	0.50	19	15	129	104	104	0	4	0	1	1	0	0	0	0	0
21	$g_-^- t_- \mid g_-^- t_- \mid t_+ t_+ \mid t_- g_-^- \mid t_- g_-^-$	9.90	0.57	17	17	129	105	105	0	4	0	0	2	0	0	0	0	0
22	$t_+ t_+ \mid t_+ t_+ \mid t_+ g_+^+ \mid t_+ t_+ \mid t_+ t_+$	16.01	0.82	17	126	127	105	109	0	1	0	3	0	0	0	0	0	0
23	$t_+ t_+ \mid t_+ t_+ \mid t_+ g_+^+ \mid t_+ g_+^+ \mid t_+ g_+^+$	13.20	0.48	18	127	127	105	108	0	3	0	2	0	0	0	0	0	0
24	$t_+ t_+ \mid t_+ t_+ \mid t_+ g_+^+ \mid t_- t_- \mid t_- t_-$	20.30	0.71	23	132	130	105	111	0	1	0	3	0	0	0	1	0	0
25	$t_+ t_+ \mid t_+ t_+ \mid t_+ g_+^+ \mid t_- g_-^- \mid t_- g_-^-$	16.88	0.48	27	127	130	105	109	0	3	0	2	0	0	0	1	0	0
26	$t_+ g_+^+ \mid t_+ g_+^+ \mid t_+ g_+^+ \mid t_+ t_+ \mid t_+ t_+$	3.16	1.57	16	128	125	111	109	0	3	0	1	0	0	0	0	0	0
27	$t_+ g_+^+ \mid t_+ g_+^+ \mid t_+ g_+^+ \mid t_+ g_+^+ \mid t_+ g_+^+$ *	0.00	1.00	15	129	125	109	109	0	0	5	5	0	0	0	0	0	0
28	$t_+ g_+^+ \mid t_+ g_+^+ \mid t_+ g_+^+ \mid t_- t_- \mid t_- t_-$	7.32	1.52	19	131	128	111	110	0	3	0	1	0	0	0	1	0	0
29	$t_+ g_+^+ \mid t_+ g_+^+ \mid t_+ g_+^+ \mid t_- g_-^- \mid t_- g_-^-$	3.58	1.22	21	128	128	111	108	0	5	0	0	0	0	0	1	0	0
30	$t_- t_- \mid t_- t_- \mid t_+ g_+^+ \mid t_+ t_+ \mid t_+ t_+$	17.13	1.52	11	130	127	105	110	0	1	0	2	1	0	0	0	0	0
31	$t_- t_- \mid t_- t_- \mid t_+ g_+^+ \mid t_+ g_+^+ \mid t_+ g_+^+$	14.38	0.80	13	131	128	105	108	0	3	0	1	1	0	0	0	0	0
32	$t_- t_- \mid t_- t_- \mid t_+ g_+^+ \mid t_- t_- \mid t_- t_-$	21.61	0.96	10	140	128	106	110	0	1	0	2	1	0	0	1	0	0
33	$t_- t_- \mid t_- t_- \mid t_+ g_+^+ \mid t_- g_-^- \mid t_- g_-^-$	18.39	0.76	12	136	128	106	109	0	3	0	1	1	0	0	1	0	0
34	$t_- g_-^- \mid t_- g_-^- \mid t_+ g_+^+ \mid t_+ t_+ \mid t_+ t_+$																	
35	$t_- g_-^- \mid t_- g_-^- \mid t_+ g_+^+ \mid t_+ g_+^+ \mid t_+ g_+^+$																	
36	$t_- g_-^- \mid t_- g_-^- \mid t_+ g_+^+ \mid t_- t_- \mid t_- t_-$																	
37	$t_- g_-^- \mid t_- g_-^- \mid t_+ g_+^+ \mid t_- g_-^- \mid t_- g_-^-$																	
38	$g_+^+ t_+ \mid g_+^+ t_+ \mid t_+ g_+^+ \mid t_+ t_+ \mid t_+ t_+$	8.32	0.82	17	126	127	103	109	0	3	0	2	0	0	0	0	0	0
39	$g_+^+ t_+ \mid g_+^+ t_+ \mid t_+ g_+^+ \mid t_+ g_+^+ \mid t_+ g_+^+$	5.27	0.44	18	126	128	103	108	0	5	0	1	0	0	0	0	0	0
40	$g_+^+ t_+ \mid g_+^+ t_+ \mid t_+ g_+^+ \mid t_- t_- \mid t_- t_-$	11.87	0.65	22	133	130	104	110	0	3	0	2	0	0	0	1	0	0
41	$g_+^+ t_+ \mid g_+^+ t_+ \mid t_+ g_+^+ \mid t_- g_-^- \mid t_- g_-^-$	8.26	0.48	25	129	130	104	110	0	5	0	1	0	0	0	1	0	0
42	$g_-^- t_- \mid g_-^- t_- \mid t_+ g_+^+ \mid t_+ t_+ \mid t_+ t_+$	9.72	1.11	13	128	128	104	110	0	3	0	1	1	0	0	0	0	0
43	$g_-^- t_- \mid g_-^- t_- \mid t_+ g_+^+ \mid t_+ g_+^+ \mid t_+ g_+^+$	6.86	0.64	14	129	128	103	109	0	5	0	0	1	0	0	0	0	0
44	$g_-^- t_- \mid g_-^- t_- \mid t_+ g_+^+ \mid t_- t_- \mid t_- t_-$	13.33	1.14	19	137	130	105	111	0	3	0	1	1	0	0	1	0	0
45	$g_-^- t_- \mid g_-^- t_- \mid t_+ g_+^+ \mid t_- g_-^- \mid t_- g_-^-$	9.85	0.85	23	132	130	105	110	0	5	0	0	1	0	0	1	0	0
46	$t_+ t_+ \mid t_+ t_+ \mid t_+ g_-^- \mid t_+ t_+ \mid t_+ t_+$	19.17	0.40	13	-101	129	104	108	0	0	1	3	0	0	1	0	0	0
47	$t_+ t_+ \mid t_+ t_+ \mid t_+ g_-^- \mid t_+ g_+^+ \mid t_+ g_+^+$	16.40	0.28	12	-101	129	104	106	0	2	1	2	0	0	1	0	0	0
48	$t_+ t_+ \mid t_+ t_+ \mid t_+ g_-^- \mid t_- t_- \mid t_- t_-$	16.93	0.51	16	-109	128	104	109	0	0	1	3	0	1	0	0	0	0
49	$t_+ t_+ \mid t_+ t_+ \mid t_+ g_-^- \mid t_- g_-^- \mid t_- g_-^-$	14.41	0.36	15	-109	128	104	107	0	2	1	2	0	1	0	0	0	0
50	$t_+ t_+ \mid t_+ t_+ \mid t_+ g_-^- \mid g_-^- t_- \mid g_-^- t_-$	16.99	0.55	12	-98	128	104	117	0	2	1	2	0	0	0	0	1	0
51	$t_+ g_+^+ \mid t_+ g_+^+ \mid t_+ g_-^- \mid t_+ t_+ \mid t_+ t_+$	6.08	0.83	12	-101	127	111	108	0	2	1	1	0	0	1	0	0	0
52	$t_+ g_+^+ \mid t_+ g_+^+ \mid t_+ g_-^- \mid t_+ g_+^+ \mid t_+ g_+^+$	2.74	0.52	11	-100	127	111	107	0	4	1	0	0	0	1	0	0	0
53	$t_+ g_+^+ \mid t_+ g_+^+ \mid t_+ g_-^- \mid t_- t_- \mid t_- t_-$	4.01	1.03	14	-107	126	111	109	0	2	1	1	0	1	0	0	0	0
54	$t_+ g_+^+ \mid t_+ g_+^+ \mid t_+ g_-^- \mid t_- g_-^- \mid t_- g_-^-$	1.05	0.73	14	-108	126	111	107	0	4	1	0	0	1	0	0	0	0
55	$t_+ g_+^+ \mid t_+ g_+^+ \mid t_+ g_-^- \mid g_-^- t_- \mid g_-^- t_-$	4.13	0.93	9	-96	126	111	107	0	4	1	0	0	0	0	0	1	0
56	$t_- t_- \mid t_- t_- \mid t_+ g_-^- \mid t_+ t_+ \mid t_+ t_+$	19.66	0.51	6	-95	129	105	107	0	0	1	2	1	0	0	0	0	0
57	$t_- t_- \mid t_- t_- \mid t_+ g_-^- \mid t_+ g_+^+ \mid t_+ g_+^+$	16.61	0.28	5	-95	128	105	106	0	2	1	1	1	0	1	0	0	0
58	$t_- t_- \mid t_- t_- \mid t_+ g_-^- \mid t_- t_- \mid t_- t_-$	18.41	0.62	10	-103	128	105	108	0	0	1	2	1	1	0	0	0	0
59	$t_- t_- \mid t_- t_- \mid t_+ g_-^- \mid t_- g_-^- \mid t_- g_-^-$	15.81	0.38	10	-103	128	105	107	0	2	1	1	1	1	0	0	0	0
60	$t_- t_- \mid t_- t_- \mid t_+ g_-^- \mid g_-^- t_- \mid g_-^- t_-$	17.93	0.56	2	-93	127	105	118	0	2	1	1	1	0	0	0	1	0
61	$t_- g_-^- \mid t_- g_-^- \mid t_+ g_-^- \mid t_+ t_+ \mid t_+ t_+$																	
62	$t_- g_-^- \mid t_- g_-^- \mid t_+ g_-^- \mid t_+ g_+^+ \mid t_+ g_+^+$																	
63	$t_- g_-^- \mid t_- g_-^- \mid t_+ g_-^- \mid t_- t_- \mid t_- t_-$																	
64	$t_- g_-^- \mid t_- g_-^- \mid t_+ g_-^- \mid t_- g_-^- \mid t_- g_-^-$																	
65	$t_- g_-^- \mid t_- g_-^- \mid t_+ g_-^- \mid g_-^- t_- \mid g_-^- t_-$																	

Table VI (*Continued*)

	hexad-conformation	E	z_0	φ_i	φ_{i+1}	$\pi-\theta'$	$\pi-\theta''_{i-1}$	$\pi-\theta''_{i+1}$	α	β	β'	γ	δ	ϵ	ζ	ξ	ρ	ψ
66	$\|g^+_+ t_+ \|g^+_+ t_+ \|t_+ g^-_+ \|t_+ t_+ \|t_+ t_+ \|$	11.18	0.35	14	-101	130	103	108	0	2	1	2	0	0	1	0	0	0
67	$\|g^+_+ t_+ \|g^+_+ t_+ \|t_+ g^-_+ \|t_+ g^+_+ \|t_+ g^+_+ \|$	8.44	0.25	14	-101	130	102	106	0	4	1	1	0	0	1	0	0	0
68	$\|g^+_+ t_+ \|g^+_+ t_+ \|t_+ g^-_+ \|t_- t_- \|t_- t_- \|$	9.41	0.40	17	-108	129	103	109	0	2	1	2	0	1	0	0	0	0
69	$\|g^+_+ t_+ \|g^+_+ t_+ \|t_+ g^-_+ \|t_- g^-_- \|t_- g^-_- \|$	6.71	0.27	17	-108	129	102	107	0	4	1	1	0	1	0	0	0	0
70	$\|g^+_+ t_+ \|g^+_+ t_+ \|t_+ g^-_+ \|g^-_- t_- \|g^-_- t_- \|$	8.12	0.42	14	-98	128	103	117	0	4	1	1	0	0	0	0	1	0
71	$\|g^-_- t_- \|g^-_- t_- \|t_+ g^+_+ \|t_+ t_+ \|t_+ t_+ \|$	12.23	0.45	10	-97	130	103	107	0	2	1	1	1	0	1	0	0	0
72	$\|g^-_- t_- \|g^-_- t_- \|t_+ g^+_+ \|t_+ g^+_+ \|t_+ g^+_+ \|$	9.25	0.26	9	-97	129	103	105	0	4	1	0	1	0	1	0	0	0
73	$\|g^-_- t_- \|g^-_- t_- \|t_+ g^+_+ \|t_- t_- \|t_- t_- \|$	11.46	0.53	13	-103	129	103	108	0	2	1	1	1	0	0	0	0	0
74	$\|g^-_- t_- \|g^-_- t_- \|t_+ g^+_+ \|t_- g^-_- \|t_- g^-_- \|$	8.75	0.36	14	-104	129	103	107	0	4	1	0	1	1	0	0	0	0
75	$\|g^-_- t_- \|g^-_- t_- \|t_+ g^+_+ \|g^-_- t_- \|g^-_- t_- \|$	9.22	0.58	8	-95	128	104	118	0	4	1	0	0	0	0	0	1	0
76	$\|t_+ t_+ \|t_+ t_+ \|g^+_+ g^+_+ \|t_+ t_+ \|t_+ t_+ \|$	14.26	1.14	130	130	127	109	109	0	2	0	2	0	0	0	0	0	0
77	$\|t_+ t_+ \|t_+ t_+ \|g^+_+ g^+_+ \|t_+ g^+_+ \|t_+ g^+_+ \|$	11.49	0.70	130	130	127	109	108	0	4	0	1	0	0	0	0	0	0
78	$\|t_+ t_+ \|t_+ t_+ \|g^+_+ g^+_+ \|t_- t_- \|t_- t_- \|$																	
79	$\|t_+ t_+ \|t_+ t_+ \|g^+_+ g^+_+ \|t_- g^-_- \|t_- g^-_- \|$																	
80	$\|t_- t_- \|t_- t_- \|g^+_+ g^+_+ \|t_+ g^+_+ \|t_+ g^+_+ \|$																	
81	$\|t_- t_- \|t_- t_- \|g^+_+ g^+_+ \|t_- t_- \|t_- t_- \|$																	
82	$\|t_- t_- \|t_- t_- \|g^+_+ g^+_+ \|t_- g^-_- \|t_- g^-_- \|$																	
83	$\|g^+_+ t_+ \|g^+_+ t_+ \|g^+_+ g^+_+ \|t_+ g^+_+ \|t^+ g^+_+ \|$	2.50	0.52	131	131	128	108	108	0	6	0	0	0	0	0	0	0	0
84	$\|g^+_+ t_+ \|g^+_+ t_+ \|g^+_+ g^+_+ \|t_- g^-_- \|t^- g^-_- \|$																	
85	$\|g^-_- t_- \|g^-_- t_- \|g^+_+ g^+_+ \|t_- g^-_- \|t_- g^-_- \|$																	
86	$\|t_+ t_+ \|t_+ t_+ \|g^+_+ g^-_- \|t_+ t_+ \|t_+ t_+ \|$	18.19	0.74	122	-98	129	109	109	1	0	1	2	0	0	1	0	0	0
87	$\|t_+ t_+ \|t_+ t_+ \|g^+_+ g^-_- \|t_+ g^+_+ \|t_+ g^+_+ \|$	15.23	0.47	121	-98	129	109	107	1	2	1	1	0	0	1	0	0	0
88	$\|t_+ t_+ \|t_+ t_+ \|g^+_+ g^-_- \|t_- t_- \|t_- t_- \|$	14.92	0.85	129	-106	127	110	109	1	0	1	2	0	1	0	0	0	0
89	$\|t_+ t_+ \|t_+ t_+ \|g^+_+ g^-_- \|t_- g^-_- \|t_- g^-_- \|$	12.41	0.53	129	-106	128	110	107	1	2	1	1	0	1	0	0	0	0
90	$\|t_+ t_+ \|t_+ t_+ \|g^+_+ g^-_- \|g^-_- t_- \|g^-_- t_- \|$																	
91	$\|t_- t_- \|t_- t_- \|g^+_+ g^-_- \|t_+ t_+ \|t_+ t_+ \|$	21.21	0.53	132	-96	131	112	107	1	0	1	2	0	0	1	1	0	0
92	$\|t_- t_- \|t_- t_- \|g^+_+ g^-_- \|t_+ g^+_+ \|t_+ g^+_+ \|$	18.56	0.36	133	-96	131	112	105	1	2	1	1	0	0	1	1	0	0
93	$\|t_- t_- \|t_- t_- \|g^+_+ g^-_- \|t_- t_- \|t_- t_- \|$																	
94	$\|t_- t_- \|t_- t_- \|g^+_+ g^-_- \|t_- g^-_- \|t_- g^-_- \|$																	
95	$\|t_- t_- \|t_- t_- \|g^+_+ g^-_- \|g^-_- t_- \|g^-_- t_- \|$	17.67	0.67	122	-100	130	109	119	1	2	1	1	0	0	0	1	1	0
96	$\|g^+_+ t_+ \|g^+_+ t_+ \|g^+_+ g^-_- \|t_+ t_+ \|t_+ t_+ \|$	9.54	0.54	122	-97	130	108	109	1	2	1	1	0	0	1	0	0	0
97	$\|g^+_+ t_+ \|g^+_+ t_+ \|g^+_+ g^-_- \|t_+ g^+_+ \|t_+ g^+_+ \|$	6.40	0.36	121	-97	129	108	107	1	4	1	0	0	0	1	0	0	0
98	$\|g^+_+ t_+ \|g^+_+ t_+ \|g^+_+ g^-_- \|t_- t_- \|t_- t_- \|$	6.38	0.61	129	-105	128	108	109	1	2	1	1	0	1	0	0	0	0
99	$\|g^+_+ t_+ \|g^+_+ t_+ \|g^+_+ g^-_- \|t_- g^-_- \|t_- g^-_- \|$	3.57	0.40	129	-105	128	109	108	1	4	1	0	0	1	0	0	0	0
100	$\|g^+_+ t_+ \|g^+_+ t_+ \|g^+_+ g^-_- \|g^-_- t_- \|g^-_- t_- \|$																	
101	$\|g^-_- t_- \|g^-_- t_- \|g^+_+ g^-_- \|t_+ t_+ \|t_+ t_+ \|$	11.78	0.46	127	-92	130	110	107	1	2	1	1	0	0	1	1	0	0
102	$\|g^-_- t_- \|g^-_- t_- \|g^+_+ g^-_- \|t_+ g^+_+ \|t_+ g^+_+ \|$	8.78	0.32	128	-92	130	110	105	1	4	1	0	0	0	1	1	0	0
103	$\|g^-_- t_- \|g^-_- t_- \|g^+_+ g^-_- \|t_- t_- \|t_- t_- \|$																	
104	$\|g^-_- t_- \|g^-_- t_- \|g^+_+ g^-_- \|t_- g^-_- \|t_- g^-_- \|$																	
105	$\|g^-_- t_- \|g^-_- t_- \|g^+_+ g^-_- \|g^-_- t_- \|g^-_- t_- \|$	7.30	0.64	124	-95	129	109	118	1	4	1	0	0	0	0	1	1	0
106	$\|t_+ t_+ \|t_+ t_+ \|g^+_- g^+_- \|t_+ t_+ \|t_+ t_+ \|$	15.63	2.06	111	111	128	109	109	0	0	2	2	0	0	2	0	0	0
107	$\|t_+ t_+ \|t_+ t_+ \|g^+_- g^+_- \|t_+ g^+_+ \|t_+ g^+_+ \|$	13.02	1.41	112	112	128	109	108	0	2	2	1	0	2	0	0	0	0
108	$\|t_+ t_+ \|t_+ t_+ \|g^+_- g^+_- \|t_- t_- \|t_- t_- \|$	18.82	0.44	111	99	130	109	108	0	0	2	2	0	1	1	0	0	0
109	$\|t_+ t_+ \|t_+ t_+ \|g^+_- g^+_- \|t_- g^-_- \|t_- g^-_- \|$	15.62	0.32	113	99	130	109	106	0	2	2	1	0	1	1	0	0	0
110	$\|t_+ t_+ \|t_+ t_+ \|g^+_- g^+_- \|g^+_+ t_+ \|g^+_+ t_+ \|$	17.84	0.52	115	94	129	109	118	0	2	2	1	0	1	0	0	1	0
111	$\|t_+ g^+_+ \|t_+ g^+_+ \|g^+_- g^+_- \|t_+ g^+_+ \|t_+ g^+_+ \|$	10.19	0.27	92	116	129	119	107	0	4	2	0	0	1	0	0	1	0
112	$\|t_+ g^+_+ \|t_+ g^+_+ \|g^+_- g^+_- \|t_- t_- \|t_- t_- \|$	15.60	0.36	94	106	130	118	107	0	2	2	1	0	0	1	0	1	0
113	$\|t_+ g^+_+ \|t_+ g^+_+ \|g^+_- g^+_- \|t_- g^-_- \|t_- g^-_- \|$	12.02	0.42	97	88	129	117	105	0	4	2	0	0	0	1	0	1	0
114	$\|t_+ g^+_+ \|t_+ g^+_+ \|g^+_- g^+_- \|g^+_+ t_+ \|g^+_+ t_+ \|$	12.82	0.28	99	99	128	117	117	0	4	2	0	0	0	0	0	2	0
115	$\|t_- t_- \|t_- t_- \|g^+_- g^+_- \|t_+ g^+_+ \|t_+ g^+_+ \|$	16.67	0.30	99	112	131	108	107	0	2	2	1	0	1	1	0	0	0
116	$\|t_- t_- \|t_- t_- \|g^+_- g^+_- \|t_- t_- \|t_- t_- \|$	22.21	0.45	104	104	132	108	108	0	0	2	2	0	0	2	0	0	0
117	$\|t_- t_- \|t_- t_- \|g^+_- g^+_- \|t_- g^-_- \|t_- g^-_- \|$	20.22	0.41	105	104	133	109	106	0	2	2	1	0	0	2	0	0	0
118	$\|g^+_+ t_+ \|g^+_+ t_+ \|g^+_- g^+_- \|t_+ g^+_+ \|t_+ g^+_+ \|$																	
119	$\|g^+_+ t_+ \|g^+_+ t_+ \|g^+_- g^+_- \|t_- g^-_- \|t_- g^-_- \|$	7.32	0.33	114	100	131	108	107	0	4	2	0	0	1	1	0	0	0
120	$\|g^-_- t_- \|g^-_- t_- \|g^+_- g^+_- \|t_- g^-_- \|t_- g^-_- \|$	11.89	0.47	109	109	134	108	108	0	4	2	0	0	0	2	0	0	0
121	$\|t_+ g^-_+ \|t_+ g^-_+ \|t_+ t_+ \|t_+ g^+_+ \|t_+ g^+_+ \|$	16.06	0.66	7	19	128	111	103	0	2	2	1	0	0	2	0	0	0
122	$\|t_+ g^-_+ \|t_+ g^-_+ \|t_- t_- \|t_+ g^+_+ \|t_+ g^+_+ \|$	15.63	0.69	-19	-13	127	110	104	0	2	2	0	1	1	1	0	0	0
123	$\|t_+ g^-_+ \|t_+ g^-_+ \|t_+ g^+_+ \|t_+ g^+_+ \|t_+ g^+_+ \|$	12.99	0.81	12	131	127	111	108	0	3	2	0	0	0	2	0	0	0
124	$\|t_+ g^-_+ \|t_+ g^-_+ \|t_- g^-_- \|t_+ g^+_+ \|t_+ g^+_+ \|$	15.21	0.60	-25	-127	128	109	109	0	3	2	0	0	1	1	1	0	0
125	$\|t_+ g^-_+ \|t_+ g^-_+ \|g^-_- t_- \|t_+ g^+_+ \|t_+ g^+_+ \|$																	
126	$\|t_+ g^-_+ \|t_+ g^-_+ \|t_+ g^-_+ \|t_+ g^+_+ \|t_+ g^+_+ \|$	25.32	0.47	1	-97	128	111	107	0	2	3	0	0	0	3	0	0	0
127	$\|t_+ g^-_+ \|t_+ g^-_+ \|g^-_+ t_+ \|t_+ g^+_+ \|t_+ g^+_+ \|$	16.89	0.25	-97	11	129	114	103	0	2	3	1	0	0	1	0	0	1
128	$\|t_+ g^-_+ \|t_+ g^-_+ \|t_- g^+_- \|t_+ g^+_+ \|t_+ g^+_+ \|$	12.47	0.43	-14	108	126	109	107	0	2	3	0	0	2	1	0	0	0
129	$\|t_+ g^-_+ \|t_+ g^-_+ \|g^-_- g^-_- \|t_+ g^+_+ \|t_+ g^+_+ \|$																	
130	$\|t_+ g^-_+ \|t_+ g^-_+ \|g^-_- g^+_- \|t_+ g^+_+ \|t_+ g^+_+ \|$																	
131	$\|t_+ g^-_+ \|t_+ g^-_+ \|g^-_+ g^-_+ \|t_+ g^+_+ \|t_+ g^+_+ \|$	20.17	0.52	-97	-109	131	116	107	0	2	4	0	0	0	2	0	0	1

Table VII
Conformational Parameters for the Six-State Scheme from Energy Calculations

η	η_0	E_η, kcal mol^{-1}
α	0.5	1.6 ± 0.2
β	0.6	0.6 ± 0.3
β'	0.6	4.2 ± 0.2
γ	0.5	5.6 ± 0.4
δ	0.6	6.2 ± 0.2
ϵ	0.7	−1.0 ± 0.3
ζ	0.7	2.0 ± 0.3
ξ	1.0	4.6 ± 0.7
ρ	0.9	2.0 ± 0.5
ψ	1.1	0.5 ± 0.3

Columns and rows are indexed in the order t_+ (+15°), t_- (−15°), g_+^+ (+130°), g_-^- (−130°), and

$$\xi = 1.0 \exp(-E_\xi/RT) \tag{17}$$

The only parameter, ξ, is relatively small, since E_ξ is estimated from the energy calculations presented above to be >4 kcal mol^{-1} (see Table VII). The estimation of energy parameters is imprecise, however, and we postpone assignment of a definite value to E_ξ. For the present it suffices to observe that $\xi \ll 1$.

The conformational preferences of PIB, reflected in eq 15 and 16, are quite different from the ones anticipated in earlier work.[5,14,19,20] The diad conformations divide into two classes, "plus" and "minus". A diad can assume $|t_+t_+|$, $|t_+g_+^+|$, $|g_+^+t_+|$, and $|g_+^+g_+^+|$ with equal probability in the "+ class". In the "− class" the signs are reversed. The zeros in $\mathbf{U}'$ dictate that a t state for a bond on one side of a quaternary carbon must be juxtaposed by a g state on the other, and vice versa. The likelihood of a "+ class" conformation being joined by a "− class" conformation, or vice versa, is given by ξ. Since $\xi \ll 1$ there will be long sequences of diad conformations belonging to one of the classes only. This matter will be pursued quantitatively after the four-state model is tested against experimental results.

The Characteristic Ratio and Its Temperature Coefficient. The characteristic ratio, $C_\infty = \lim_{n\to\infty}(\langle r^2\rangle_0/nl^2)$, was calculated using the four-state scheme according to well-established methods.[25,41] Values of $\pi - \theta' = 124°$ and $\pi - \theta'' = 109°$ are indicated by the results in Table VI. These angles together with $E_\xi = 4.6$ kcal mol^{-1} and eq 15–17 give $C_\infty = 7.16$ and d ln $C_\infty/dT = -0.02 \times 10^{-3}$ K^{-1}. The computed value of C_∞ exceeds experimental results (Table I) by ca. 5%, and the absolute value of the temperature coefficient is somewhat smaller than experiments indicate. The calculation of C_∞ is most sensitive to θ', and d ln C_∞/dT is most sensitive to E_ξ: $\partial C_\infty/\partial\theta' = +0.291$ deg^{-1} whereas $\partial C_\infty/\partial E_\xi = +0.002$ mol kcal^{-1} and $10^3\,\partial^2 \ln C_\infty/\partial T\partial\theta' = 0.0004$ K^{-1} deg^{-1} whereas $10^3\,\partial^2 \ln C_\infty/\partial T\partial E_\xi = +0.012$ K^{-1} mol kcal^{-1}. The effects of these two parameters are mutually independent. To bring C_∞ into the range of the experimental values it is sufficient to change θ' by 1°, i.e., to take $\pi - \theta' = 123°$. This adjusted value was used in all succeeding calculations. The effect of the variation of E_ξ is shown in Table VIII. As E_ξ decreases from large positive values, the temperature coefficient decreases also and becomes more and more negative; it reaches a minimum of -0.17×10^{-3} K^{-1} at $E_\xi = 1.25$ kcal mol^{-1}. Comparison of the values in Table VIII with the experimental results from Table I and with the results of calculations in Table VII supports a value of $E_\xi \simeq 3$ kcal mol^{-1}. Equation 17 can then be written as

$$\xi = 1.0 \exp(-1500/T) \tag{18}$$

Table VIII
Calculated Characteristic Ratio and Its Temperature Coefficient, at 300 K[a]

E_ξ, kcal mol^{-1}	C_∞	10^3 d ln C_∞/dT, K^{-1}	$10^3\partial^2 \ln C_\infty/\partial T\,\partial E_\xi$, K^{-1} mol kcal^{-1}
$\to\infty$	6.83	0	0
4.6	6.82	−0.02	+0.01
3.0	6.81	−0.05	+0.05
2.0	6.75	−0.12	+0.09
1.2_5	6.60	−0.17	-0.00_4

[a] $\pi - \theta' = 123°$, $\pi - \theta'' = 109°$; RIS conformational states as specified in the text.

At 300 K, $\xi \simeq 0.007$.

It is noteworthy that for a freely rotating chain with the same bond angles, where $C_\infty = (1 + \cos\theta')(1 + \cos\theta'')/(1 - \cos\theta'\cos\theta'')$,[42] the characteristic ratio would be only 2.5.

Partition Function and Conformation Probabilities. The conformational partition function for the PIB chain of x units is given by

$$Z = \mathbf{U}_0[\mathbf{U}^{(2)}]^{x-1}\mathbf{U}_x \tag{19}$$

where $\mathbf{U}_0 = [1\ 0\ 0\ 0]$ (the chain being initiated arbitrarily in the "+ class") and $\mathbf{U}_x = \mathrm{col}(1,1,1,1)$. $\mathbf{U}^{(2)}$ is the diad matrix

$$\mathbf{U}^{(2)} \equiv \mathbf{U}'\mathbf{U}'' = \mathbf{U}''\mathbf{U}' = \begin{bmatrix} 1 & \xi & 1 & \xi \\ \xi & 1 & \xi & 1 \\ 1 & \xi & 1 & \xi \\ \xi & 1 & \xi & 1 \end{bmatrix} \tag{20}$$

It has two nonzero eigenvalues, $\lambda_1 = 2(1 + \xi)$ and $\lambda_2 = 2(1 - \xi)$. The eigenvector matrix $\mathbf{A}$ associated with $\mathbf{U}^{(2)} = \mathbf{ADA}^{\mathrm{T}}$, where $\mathbf{D} = \mathrm{diag}(\lambda_1,\lambda_2,0,0)$, is

$$\mathbf{A} = \frac{1}{2}\begin{bmatrix} 1 & 1 & 1 & 1 \\ 1 & -1 & 1 & -1 \\ 1 & 1 & -1 & -1 \\ 1 & -1 & -1 & 1 \end{bmatrix} \tag{21}$$

Substitution of $\mathbf{U}^{(2)} = \mathbf{ADA}^{\mathrm{T}}$ into eq 19 yields, for *all* values of x,

$$Z = [2(1 + \xi)]^{x-1} \tag{22}$$

The matrix of a priori probabilities for the conformations within a diad, $\mathbf{P}''$, is, according to the methods of ref 40,

$$\mathbf{P}'' = \frac{1}{8}\begin{bmatrix} 1+\Delta & 0 & 1+\Delta & 0 \\ 0 & 1-\Delta & 0 & 1-\Delta \\ 1+\Delta & 0 & 1+\Delta & 0 \\ 0 & 1-\Delta & 0 & 1-\Delta \end{bmatrix} \tag{23}$$

with

$$\Delta = [(1 - \xi)/(1 + \xi)]^{x/2} \tag{24}$$

Again, the t_+ conformation was chosen for the first skeletal bond in the chain; for t_- the signs in the matrix of eq 23 would be reversed. For $\xi > 0$ and long chains, this matrix simplifies to

$$\mathbf{P}'' = \mathbf{U}''/8 \qquad \xi > 0 \text{ and } x \to \infty \tag{25}$$

and every diad conformation in a long chain has an a priori probability of $^1/_8$. The a priori probabilities for a single bond are just the column sums of $\mathbf{P}''$, and for long chains ($\xi > 0$) every bond conformation has an a priori probability of $^1/_4$. Convergence of eq 23 to eq 25 is quite slow, however; for $\xi = 0.007$ (i.e., at 300 K), Δ becomes less than 0.01 only for $x > 660$.

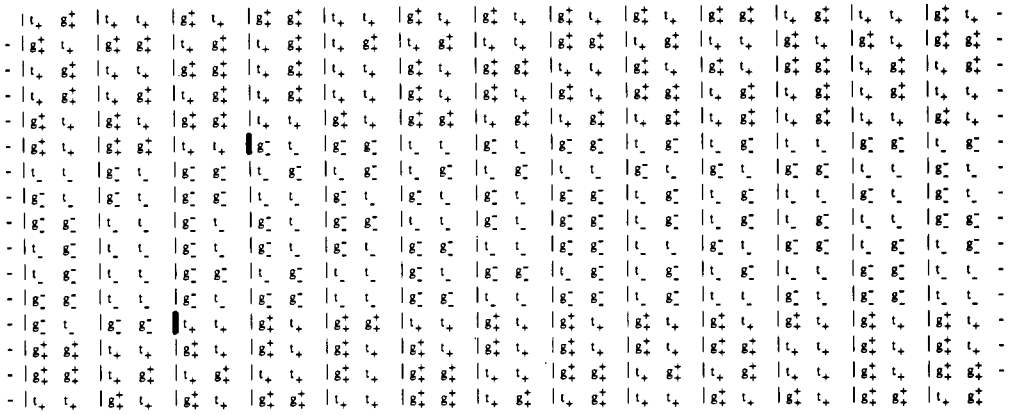

Figure 3. A simulated sequence of conformations of 208 diads, with $\xi = 0.007$, illustrating the stochastic nature of PIB conformations. Heavy vertical lines mark reversals between + and − classes.

The matrix $\mathbf{P}'$ of a priori probabilities for the conformations around a quaternary carbon atom is

$$\mathbf{P}' = \frac{1}{4(1+\xi)} \times \begin{bmatrix} 0 & 0 & 1+\Delta' & \xi(1+\Delta') \\ 0 & 0 & \xi(1-\Delta') & 1-\Delta' \\ 1+\Delta' & \xi(1-\Delta') & 0 & 0 \\ \xi(1+\Delta') & 1-\Delta' & 0 & 0 \end{bmatrix} \quad (26)$$

with

$$\Delta' = [(1-\xi)/(1+\xi)]^{x/2-1} \quad (27)$$

For $\xi > 0$ and long chains this simplifies to

$$\mathbf{P}' = \mathbf{U}'/4(1+\xi) \qquad \xi > 0 \text{ and } x \to \infty \quad (28)$$

In general,[40] the *conditional* probability $q_{\tau\eta;i}$ that bond i is in state η while bond $i-1$ is in state τ is given by the *a priori* probability $p_{\tau\eta;i}$ of this situation divided by the *a priori* probability $p_{\tau;i-1}$ for bond $i-1$ to be in state τ. It is straightforward to obtain the matrices $\mathbf{Q}$ of conditional probabilities from $\mathbf{P}'$ and $\mathbf{P}''$ above. For long chains

$$\mathbf{Q}'' = \mathbf{U}''/2 \qquad \xi > 0 \text{ and } x \to \infty \quad (29)$$

and

$$\mathbf{Q}' = \mathbf{U}'/(1+\xi) \qquad \xi > 0 \text{ and } x \to \infty \quad (30)$$

The forms of $\mathbf{Q}'$ and $\mathbf{Q}''$ are simple and allow one to calculate the average length of a sequence of regularly conformed units in a long PIB chain. The probability that a given diad assumes the specified conformation is the product of the probabilities, $1/(1+\xi)$ and $^1/_2$, that the first and second bonds of the next diad occur in the required states. The probability of termination of the sequence is the sum of the probabilities that it is terminated at the first bond of the next diad, $\xi/(1+\xi)$, or at the second bond, $1/2(1+\xi)$. Therefore, the probability that a regular sequence in a long chain is exactly y diads in length is

$$p(y) = [1/2(1+\xi)]^{y-1}[\xi/(1+\xi) + 1/2(1+\xi)] = (1+2\xi)[2(1+\xi)]^{-y} \qquad x \to \infty \quad (31)$$

It follows that the average sequence length is

$$\langle y \rangle = 2(1+\xi)/(1+2\xi) \qquad x \to \infty \quad (32)$$

Thus, for $\xi = 0.007$, $\langle y \rangle = 1.986$. The deviation from 2 is due to the occasional transition between classes.

The average length of a sequence of units in one class of conformations ($y\pm$) is

$$\langle y\pm \rangle = (1+\xi)/\xi \qquad x \to \infty \quad (33)$$

For $\xi = 0.007$, at 300 K, $\langle y\pm \rangle$ is 144.

A conformational sequence of 208 diads generated from eq 29 and 30 using $\xi = 0.007$ is displayed in Figure 3.

Registry No. Polyisobutylene, 9003-27-4; 2,2,4,4-tetramethylpentane, 1070-87-7; 2,2,4,4,6,6-hexamethylheptane, 34701-49-0.

References and Notes

(1) Fuller, C. S.; Frosch, C. J.; Pape, N. R. *J. Am. Chem. Soc.* **1940**, *62*, 1905–1913.
(2) Liquori, A. M. *Acta Crystallogr.* **1955**, *8*, 345–347.
(3) Bunn, C. W.; Holmes, D. R. *Faraday Discuss. Chem. Soc.* **1958**, *25*, 95–103.
(4) Wasai, G.; Saegusa, T.; Furukawa, J. *Makromol. Chem.* **1965**, *86*, 1–8.
(5) Allegra, G.; Benedetti, E.; Pedone, C. *Macromolecules* **1970**, *3*, 727–735.
(6) Tanaka, T.; Chatani, Y.; Tadokoro, H. *J. Polym. Sci., Polym. Phys. Ed.* **1974**, *12*, 515–531.
(7) Kusanagi, H.; Tadokoro, H.; Chatani, Y. *Polym. J.* **1977**, *9*, 181–190.
(8) Fox., T. G.; Flory, P. J. *J. Am. Chem. Soc.* **1951**, *73*, 1909–1914.
(9) Krigbaum, W. R.; Flory, P. J. *J. Polym. Sci.* **1953**, *9*, 37–51.
(10) Matsumoto, T.; Nishioka, N.; Fujita, H. *J. Polym. Sci., Polym. Phys. Ed.* **1972**, *10*, 23–42.
(11) Cifferi, A.; Hoeve, C. A. J.; Flory, P. J. *J. Am. Chem. Soc.* **1961**, *83*, 1015–1022.
(12) Allen, G.; Gee, G.; Kirkham, M. C.; Price, C.; Padget, J. *J. Polym. Sci., Part C* **1968**, *No. 23*, 201–204.
(13) Mark, J. E.; Thomas, G. B. *J. Phys. Chem.* **1966**, *70*, 3588–3590.
(14) Ptitsyn, O. B.; Sharanov, Iu. A. *Zh. Tekh. Fiz.* **1957**, *27*, 2744–2761, 2762–2773; *Soviet Phys.-Tech. Phys. (Engl. Transl.)* **1959**, *2*, 2544–2560, 2561–2571.
(15) Birshtein, T. M.; Ptitsyn, O. B.; Sokolova, E. A. *Vysokomol. Soedin, Ser. A* **1959**, *1*, 852–856; Abstract in *Polymer Sci. USSR (Engl. Transl.)*, p 333–334.
(16) Hoeve, C. A. J. *J. Chem. Phys.* **1960**, *32*, 888–893.
(17) DeSantis, P.; Giglio, E.; Liquori, A. M.; Ripamonti, A. *J. Polym. Sci., Part A* **1963**, *1*, 1383–404.
(18) Haegele, P. C.; Pechhold, W. *Kolloid-A. A. Polym.* **1970**, *241*, 977–984.
(19) Boyd, R. H.; Breitling, S. M. *Macromolecules* **1972**, *5*, 1–7.
(20) Flory, P. J.; Sundararajan, P. R.; DeBolt, L. C. *J. Am. Chem. Soc.* **1974**, *96*, 5015–5024.
(21) Tanaka, A.; Ishida, Y. *J. Polym. Sci., Polym. Phys. Ed.* **1974**, *12*, 1283–1302.
(22) Abe, A.; Jernigan, R. L.; Flory, P. J. *J. Am. Chem. Soc.* **1966**, *88*, 631–639.
(23) Chang, S.-J.; McNally, D.; Shary-Tehrany, S.; Hickey, M. J.; Boyd, R. H. *J. Am. Chem. Soc.* **1970**, *92*, 3109–3118.
(24) Suter, U. W. *J. Am. Chem. Soc.* **1979**, *101*, 6481–6496.
(25) Flory, P. J. "Statistical Mechanics of Chain Molecules"; Interscience: New York, 1969; p 135.
(26) Fletcher, R.; Powell, M. J. D. *Comput. J.* **1963**, *6*, 163.
(27) Hillstrom, K. Argonne National Laboratory, Technical Memorandum No. 297, 1976, Subroutine GQBFGS in AMDLIB, 1976, Argonne, IL.
(28) Fletcher, R. A.E.R.E. Report No. R-7125, 1972, Harwell, England, Subroutine VA10A in Harwell Subroutine Library, 1972, Harwell, England.

(29) Benedetti, E.; Pedone, C.; Allegra, G. *Macromolecules* **1970**, *3*, 16–19.
(30) The actual computational effort is much less than the number of iterative steps multiplied by the effort for the first minimization, since the final estimate of the Hessian matrix found in the minimization in one step is used as an initial estimate for the Hessian in the next step (the estimation of this matrix being the most laborious part in the minimization), and this estimate becomes rapidly better as the iterative scheme proceeds, making the minimizations in the iterative scheme successively more and more efficient.
(31) Flory, P. J. "Principles of Polymer Chemistry", 10th ed.; Cornell University Press: Ithaca, NY, 1978; p 254.
(32) Richardson, J. W.; Parks, G. S. *J. Am. Chem. Soc.* **1939**, *61*, 3543–3546.
(33) Evans, A. G.; Polanyi, M. *Nature (London)* **1943**, *152*, 738.
(34) Parks, G. S.; Mosher, H. P. *J. Polym. Sci., Polym. Chem. Ed.* **1963**, *1*, 1979–1984.
(35) Biddlup, R. H.; Plesch, P. H.; Rutherford, P. P. *Polymer* **1960**, *1*, 521.
(36) Miyazawa, T. *J. Polym. Sci.* **1961**, *55*, 215–231.
(37) In our notation, Miyazawa's formulas are

$$\cos(\alpha/2) = \cos\left(\frac{\varphi_i + \varphi_{i+1}}{2}\right)\cos(\theta'/2)\cos(\theta''/2) + \cos\left(\frac{\varphi_i - \varphi_{i+1}}{2}\right)\sin(\theta'/2)\sin(\theta''/2)$$

and

$$d = 2l\sin\left(\frac{\varphi_i + \varphi_{i+1}}{2}\right)\cos(\theta'/2)\cos(\theta''/2)/\sin(\alpha/2)$$

(38) Abramowitz, M.; Stegun, I. A. "Handbook of Mathematical Functions"; *Natl. Bur. Stand. (U.S.) Circ.*, p 884.
(39) Suter, U. W.; Flory, P. J. *Macromolecules* **1975**, *8*, 765–776.
(40) p 73 ff of ref 25.
(41) Flory, P. J. *Macromolecules* **1974**, *7*, 381–392.
(42) Flory, P. J.; Mandelkern, L.; Kinsinger, J. B.; Shultz, W. B. *J. Am. Chem. Soc.* **1952**, *74*, 3365–3367.

Configuration of the Polyisobutylene Chain according to Neutron and X-ray Scattering

Hisao Hayashi† and Paul J. Flory*

IBM Research Laboratory, San Jose, California 95193

George D. Wignall

National Center for Small-Angle Scattering Research, Oak Ridge National Laboratory, Oak Ridge, Tennessee 37830. *Received January 17, 1983*

ABSTRACT: The dimensions and configurations of polyisobutylene (PIB) chains in the bulk and in solution have been investigated by neutron and X-ray scattering at small and at intermediate angles. Measurements in bulk were carried out by neutron scattering on protonated PIB (PIB-H) dispersed in matrices consisting either of fully deuterated PIB-d_8 or of the hexadeuterio polymer, PIB-d_6, in which only the methyl groups are deuterated. Neutron scattering from PIB-H dissolved in benzene-d_6 at 26.4 °C provided results in a Θ-solvent, and X-ray scattering measured in *n*-heptane allowed observations on the configurations as represented by carbon scattering centers. The *z*-average radii of gyration, $\langle s^2\rangle_z^{1/2}$, were calculated from Zimm plots in the Guinier region. Values of $\langle s^2\rangle_z^{1/2}$ measured in the bulk (75 ± 5 Å) and in the Θ-solvent (77 ± 5 Å) are in good agreement. Results of scattering measurements at intermediate angles were compared by use of Kratky plots on an absolute scale, i.e., $F_x(\mu) = (x+1)\mu^2P(\mu)$ vs. μ, where μ is the magnitude of the scattering vector, $x+1$ the number of monomer units per chain, and $P(\mu)$ the normalized scattering function. The scattering curves for PIB-H observed in the PIB-d_8 matrix and in the Θ-solvent are in excellent accord in the range of $0 < \mu < 0.6$ Å^{-1}. These results demonstrate that the configuration in the bulk is virtually the same as in a Θ-solvent. The experimental data were compared also with theoretical scattering functions calculated on the basis of the conformational analysis of random PIB chains presented in the preceding paper. Five absolute Kratky functions $F_x(\mu)$ were calculated for scattering points consisting of (i) all eight protons, (ii) six methyl protons, (iii) two methylene protons, (iv) all four carbon atoms, and (v) only the substituted carbons in the monomer unit. These five functions differ appreciably for larger values of μ, indicating the importance of a proper choice of scattering points when calculations are compared with experimental curves. The first function (i) was compared with the experimental neutron scattering curves for PIB-H in the PIB-d_8 matrix and in the Θ-solvent, the second (ii) with that observed in the PIB-d_6 matrix, and the fourth (iv) with the X-ray scattering curve observed in solution. Close agreement throughout the range of μ covered by the experiments confirms the conformational analysis of PIB and demonstrates randomness of configurations in the bulk down to distances of ca. 10 Å.

Introduction

Recent applications of neutron scattering to studies of polymers[1] have provided much valuable information inaccessible by other methods. In particular, elastic scattering experiments with isotopically labeled polymers have succeeded in characterizing chain configurations in condensed systems such as bulk polymers and concentrated solutions. These experiments take advantage of the characteristics of hydrogen and deuterium whereby they differ in scattering length for neutrons while conferring closely similar thermodynamic properties on the polymer. A protonated polymer dispersed in a deuterated matrix (or vice versa) yields particle scattering that is unaffected by intermolecular interference and hence provides information on its intramolecular configurations. This method, applied to small-angle scattering by various polymers,[2-9]

† On leave from the Department of Polymer Chemistry, Kyoto University, Kyoto 606, Japan.

0024-9297/83/2216-1328$01.50/0